Channel Temperature Estimates for Microwave AlGaN/GaN Power HEMTS on SiC and Sapphire

by

Jon C. Freeman

NASA Glenn Research Center

MS 54-5, 21000 Brookpark Rd. Cleveland, Ohio 44135

jon.c.freeman@nasa.gov

ABSTRACT

A key parameter in the design trade-offs made during AlGaN/GaN HEMTs development is the channel temperature. An accurate determination can generally only be found using detailed software; However, a quick estimate is always helpful, as it speeds up the design cycle. This paper gives a simple technique to estimate the channel temperature of a generic AlGaN/GaN HEMT on SiC or Sapphire, while incorporating the temperature dependence of the thermal conductivity. The procedure is validated by comparing its predictions with the experimentally measured temperatures in devices presented in three recently published articles.

Keywords:

I. Introduction

At the present time many research groups are studying AlGaN/GaN HEMTs for high frequency (up to Ka-band), high power applications [1], [2]. The large power density generated in power amplifiers causes considerable self-heating, and a reasonably accurate estimate of the channel temperature is often desired. Knowledge of the temperature is essential as both the carrier mobility and reliability suffer. The mobility reduces with increasing temperature as (1/T)**2.3, with resulting decrease in DC and rf performance [3]. Both short and long term reliability are key parameters, which also reflect the need to rapidly calculate the temperature profile in a particular design.

A self-consistent solution for the thermal field in a particular device can be obtained using either 2-D or 3-D simulators available in the SILVACO code [4]. Some recent analytical articles [5], [6], [7] give techniques to quickly ascertain junction temperatures under certain conditions. This article demonstrates a procedure to estimate the channel temperature in AlGaN/GaN HEMTs on either SiC or Sapphire, using simple analytic expressions. The device is modeled using the thermal resistance method, while considering the temperature dependence of the thermal conductivity.

II. Analysis Procedure

A generic HEMT is shown in Figures 1 and 2. The thermal conductivities for the many material layers, were determined by making rough averages of the values reported in the literature. Figure 3 presents the simple thermal resistance stack. The heat sources are thin strips in the gate-drain channels. The technique consists of determining the thermal footprints of the heat sources at each successive lower layer, and then determining the thermal resistance.

In principle, in any heat transport problem, one solves for the temperature field from the heat flow equation

$$\nabla \cdot \{ \kappa_i(T) \nabla T \} = -P \tag{1}$$

Where $\kappa_i(T)$ is the temperature dependent thermal conductivity in the i-th layer, T is the temperature, and P is the dissipated power density. The equation is altered by defining an equivalent artificial temperature via the Kirchhoff transformation

$$T_i^e = T_o + \frac{1}{\kappa_i(T_o)} \int_{T_o}^{T} \kappa_i(\xi) d\xi \tag{2}$$

where T_o is the reference temperature, T_i^e is the transformed temperature in the i-th layer, and T is the real temperature there. The transform linearizes eq.(1) with the result

$$\kappa_i(T_o) \nabla^2 T_i^e = -P \tag{3}$$

Our first task is to determine analytical expressions for the temperature dependent thermal conductivities of the GaN, SiC, and Sapphire layers. We have not found an analytical expression for the thermal conductivity of GaN, but from [8], [9] we may assume it to be

$$\kappa_{GaN}(T) = 1.6 \left(\frac{300}{T} \right)^{1.4} \frac{W}{cm \cdot K} \tag{4}$$

where we have assumed the behavior of GaN is similar to that of GaP. For SiC we choose [10]

$$\kappa_{SiC}(T) = 3.4 \left(\frac{300}{T} \right)^{1.5} \frac{W}{cm \cdot K} \tag{5}$$

and for Sapphire we use the result from [11]

$$\kappa(T) = \frac{73.9}{T - 159} \approx \frac{(.49)(300)}{T} \frac{W}{cm \cdot K} \tag{6}$$

The thermal resistance for a stripe is from [12], see Figure 4.

$$R_{TH} = \frac{1}{\kappa}\int_0^W \frac{dz}{A(z)} = \frac{1}{4\kappa l_x}\,\frac{1}{(\gamma_e \tan\alpha - \tan\beta)}\,\ln\left[\frac{l_x + W\tan\alpha}{l_x + W\frac{\tan\alpha}{\gamma_e}}\right] \tag{7}$$

where

$$(\tan\alpha)_i = (1 - l_{x_m})\left.\frac{W_m + \frac{\rho_s}{1+\rho_s} l_{x_m}}{W_m + \frac{1}{1+\rho_s} l_{x_m}}\right|_i \tag{8}$$

$$(\tan\beta)_i = \left(1 - l_{x_m}\frac{\gamma_e}{\gamma_s}\right)\left.\frac{W_m + \frac{\rho_s}{1+\rho_s} l_{x_m}\gamma_e}{W_m + \frac{1}{1+\rho_s} l_{x_m}\gamma_e}\right|_i \tag{9}$$

$$W_m = \frac{W}{L_x},\quad \gamma_s = \frac{L_y}{L_x},\quad \gamma_e = \frac{l_y}{l_x},\quad l_{x_m} = \frac{l_x}{L_x},\quad \rho_s = \frac{\kappa_i}{\kappa_{i+1}}$$

In regions where the thermal fluxes intersect, the formulas from [13] (with typos removed) are applicable.

$$R_{TH}\, Z\, \kappa = \frac{n}{\pi\left[\frac{2(n-1)}{\ln M} - \frac{(n-2)}{\ln P}\right]} \tag{10}$$

where n = the number of fingers
Z = total gate width

and

$$M = \frac{2\sqrt{u}+1}{\sqrt{u}-1},\qquad u = \frac{\cosh\left[\frac{\pi}{4}\left(\frac{S+L}{F}\right)\right]}{\cosh\left[\frac{\pi}{4}\left(\frac{S-L}{F}\right)\right]} \tag{11}$$

$$P = 2\sqrt{\frac{\operatorname{sech}\left(\frac{\pi L}{4F}\right)+1}{\operatorname{sech}\left(\frac{\pi L}{4F}\right)-1}} \tag{12}$$

The step-by-step procedure starts with the heat sources on the top surface; which are strips with the short side dimension being that of the gate, or the gate-drain spacing. Using eqns. (8) and (9), to determine the flow pattern; the footprint on the next lower surface is determined. The thermal resistances may be obtained from Eq.(10) which is applicable for either a single strip, or multiple ones; whereas eq.(7) is restricted to single ones. With the flow patterns and resistances of each layer determined, the calculation continues by starting at the assumed sink temperature and working upward through the layers. The change in temperature across a layer is given by

$$\Delta T_i = \theta_i P_{DISS} \tag{13}$$

ΔT_i = the temperature rise

θ_i = the thermal resistance

P_{DISS} = the power dissipated

The actual temperatures are used in the layers with constant thermal conductivity, and the artificial ones are used in the GaN, SiC, and Sapphire layers. For the GaN, SiC, and Sapphire layers, the actual temperature is determined from the transformed one by

$$T_A(GaN) = \left\{ \frac{[T^e - T_0(3.5)](-.4)}{T_0^{1.4}} \right\}^{-2.5} \tag{14}$$

$$T_A(SiC) = \left\{ \frac{[T^e - T_0(3)](-.5)}{T_0^{1.5}} \right\}^{-2} \tag{15}$$

$$T_A(Sapphire) = T_0 \exp\left[\frac{T_e - T_0}{T_0} \right] \tag{16}$$

While the Kirchhoff transform gives a linear equation, the nonlinearity inherent in eq.(1) is now pushed into the boundary conditions. For a layered structure such as a HEMT, this can be troublesome when attempting to write simple code [14]. In layered structures, the artificial temperature will generally have jumps across interfaces. However, as stated in [14], these jumps can be eliminated by choosing the analytical forms for the conductivities of the layers, $\kappa_i(T)$, in such a way that their ratio is independent of temperature. This lead us to assume the forms given above. For GaN and SiC, the ratio of the conductivities is

$$\frac{\kappa_{GaN}(T)}{\kappa_{SiC}(T)} = .266\, T^{0.1} \approx \text{constant} \tag{17}$$

or a 6% change over a 200°C range.

III. Comparison with Experimental Data

Temperature measurements on AlGaN/GaN HEMTs on both SiC or Sapphire were made using Raman spectroscopy [15], [16]. For a single gate device [15] on SiC, the measured temperature on the top surface was 180°C. We choose the heat source to be 1μ wide (the gate width), and the GaN thickness was F = 1.2μ. Using eq.(10) for n = 1 gives $\theta \approx \kappa$ = 0.587. Assume $\kappa(T)$ = 1.6 (the 300 K value) as we don't know the actual temperature at the interface yet. This will underestimate the final channel temperature. We find $\theta(GaN) = 18.35$ K/W. Using eqns.(7) & (8) we find the footprint is 3.086μ by 200.2μ. Repeat eq.(10) and obtain $\theta \approx \kappa$ = 2.02, and $\theta(SiC) = 29.73$ K/W. The dissipated power is 1.754 W, which yields $\Delta T(SiC)$ = 52 K, $\Delta T(GaN)$ = 32.2 K. Using eq.(15) gives $T(SiC, actual)$ = 86.6°C. Then in the GaN, T^e = 359.6 + 32.2 = 391.8 K, or $T(GaN, actual)$ = 121°C. The measured value was 124°C ± 5°C. We can make a correction for $\theta(GaN)$ by using κ(359.6 K) = 1.24. Then $\theta(GaN)$ = 23.7 K/W and the temperature becomes 132°C. The 3-D model used in [15] assumed constant κ and predicted T = 99°C. For the sapphire substrate case we choose L = 4μ (gate length), $\kappa(sapp, 300K)$ = 0.49; then $\theta(GaN)$ = 8.35 K/W, $\theta(SiC)$ = 180.5 K/W, $\Delta T(sapp)$ = 117.3 K, $\Delta T(GaN)$ = 5.4 K. Then the temperature on the top surface becomes 176°C. The measured value was 180°C; and the 3-D model predicted 140°C.

An 8-gate device on SiC (for 2-4 GHz amplifier applications) was measured in [16], and the thermal profile is shown in Figure 5 a). Using the outlined procedure one obtains T = 179°C (shown dotted); which agrees favorably with the average of the measurement.

Measurements using nematic liquid crystal thermography on a 2-gate device on sapphire were performed in [17]; see Figure 5 c). Our computations yielded 59°C (lower curve) and 76.5°C for the upper case.

IV. Conclusions

We have demonstrated an easy method to estimate the channel temperature in an AlGaN/GaN HEMT for microwave amplifiers. With accurate expressions for the temperature dependent thermal conductivity and using previously published equations for the thermal resistance of parallel stripes, one calculates a temperature that is within 5-10% of the true average channel temperature.

Acknowledgement

I wish to acknowledge Dr. Sam Alterovitz's helpful discussions during this investigation.

REFERENCES

[1] L. F. Eastman and U. K. Mishra, "The Toughest Transistor Yet," IEEE Spectrum, May 2002, pp 28-33.

[2] R. J. Trew, "Transistors for Microwave Power Amplifiers," IEEE Microwave Magazine, 1, March 2000, pp 46-54.

[3] E. Kohn, I. Daumiller, M. Kunze, M. Neuburger, M. Seyboth, T. Jenkins, J. Sewell, J. Van Norstrand, Y. Smorchkova, and U. Mishra, "Transient Characteristics of GaN-Based Heterostructure Field-Effect Transistors," IEEE Trans. Microwave Theory Tech., vol. MTT-51, pp 634-642, Feb. 2003.

[4] SILVACO Data Systems, N. Chelmsford, Mass.

[5] F. Masana, "A Closed Form Solution of Junction to Substrate Thermal Resistance in Semiconductor Chips," IEEE Trans. Components, Packaging, and Manufacturing Tech.-Part A 19, Dec. 1966, pp 539-545.

[6] N. Rinaldi, "Thermal analysis of solid-state devices and circuits: an analytical approach," Solid-State Electronics, 44, 2000, pp 1789-1798.

[7] M. Pesare, A. Giorgio and A. Perri, "Electrothermal model of GaAs FET devices for fast PC implementation," IEE Proc.-Circuits Devices Systems, 148, Feb. 2001, pp 40-44.

[8] V. Palankovski and S. Silberherr, "Themal Models for Semiconductor Device Simulation,"The Third European Conference on High Temperature Electronics, HITEN 99," July 7, 1999, pp 25-28.

[9] J. L. Hudgins, G. S. Simin, E. Santi, and M. Asif Khan, "An Assessment of Wide Bandgap Semiconductors for Power Devices," IEEE Transactions on Power Electronics, Vol. 18, May 2003, pp 907- 914.

[10] A. S. Royet, T. Ouisse, B. Cabon, O. Noblanc, C. Arnodo, and C. Brylinski "Self-Heating Effects in Silicon Carbide MESFETs," IEEE Transaction on Electron Devices, Vol. 47, November 2000, pp 2221-2227.

[11] M. Yamada, K. Nambu, Y. Itoh, and K. Yamamoto, "Raman microprobe study on temperature distribution during CW laser heating of silicon on sapphire," J. Appl. Phys. 59, Feb. 1986, pp 1350-1354.

[12] F. N. Masana, "A new approach to the dynamic thermal modeling of semiconductor packages," Microelectronics Reliability, 41, 2001, pp 901-912.

[13] H. F. Cooke, "Precise technique finds FET thermal Resistance," Microwaves & RF, Aug. 1986, pp 85-87.

[14] F. Bonani and G. Ghione, "On the application of the Kirchhoff transformation to the steady-state thermal analysis of semiconductor devices with temperature-dependent and piecewise inhomogeneous thermal conductivity," Solid-State Electronics, 38, No. 7, 1995, pp 1409-1412.

[15 M. Kuball, et al, "Measurement of Temperature in Active High-Power AlGaN/GaN HFETs Using Raman Spectroscopy," IEEE Electron Device Letters, Vol. 23, Jan. 2002, pp 7-9.

[16] M. Kuball, S. Rajasingam, A. Sarua, M Uren, T. Martin, B. Hughes, K. Hilton, and R. Balmer, "Measurement of temperature distribution in multifinger AlGaN/GaN heterostructure field-effect transistors using micro-Raman spectroscopy," Applied Physics Letters, 82, Jan. 2003, pp 124-126.

[17] J. Park, M. W. Shin, and C. C. Lee, "Thermal Modeling and Measurement of GaN-Based HFET Devices, IEEE Electron Device Letters, Vol. 24, July 2003, pp 424-426.

Figure Captions

1. Schematic of an 8-gate HEMT for Ka-band operation.
2. Approximate layers of material with average, or ranges, of thermal conductivities.
3. Device of Figure 1 on an approximate MMIC chip. The thermal resistance of each layer is calculated separately ($\theta = R_{TH}$).
4. Geometry for calculating thermal resistance for a single stripe a), or parallel stripes b).
5. Comparison with Kuball [16] and Park [17]. Part a) shows measurement (solid) [16] and estimate (dotted). Part b) shows estimate (dotted) for two power dissipation cases [17].

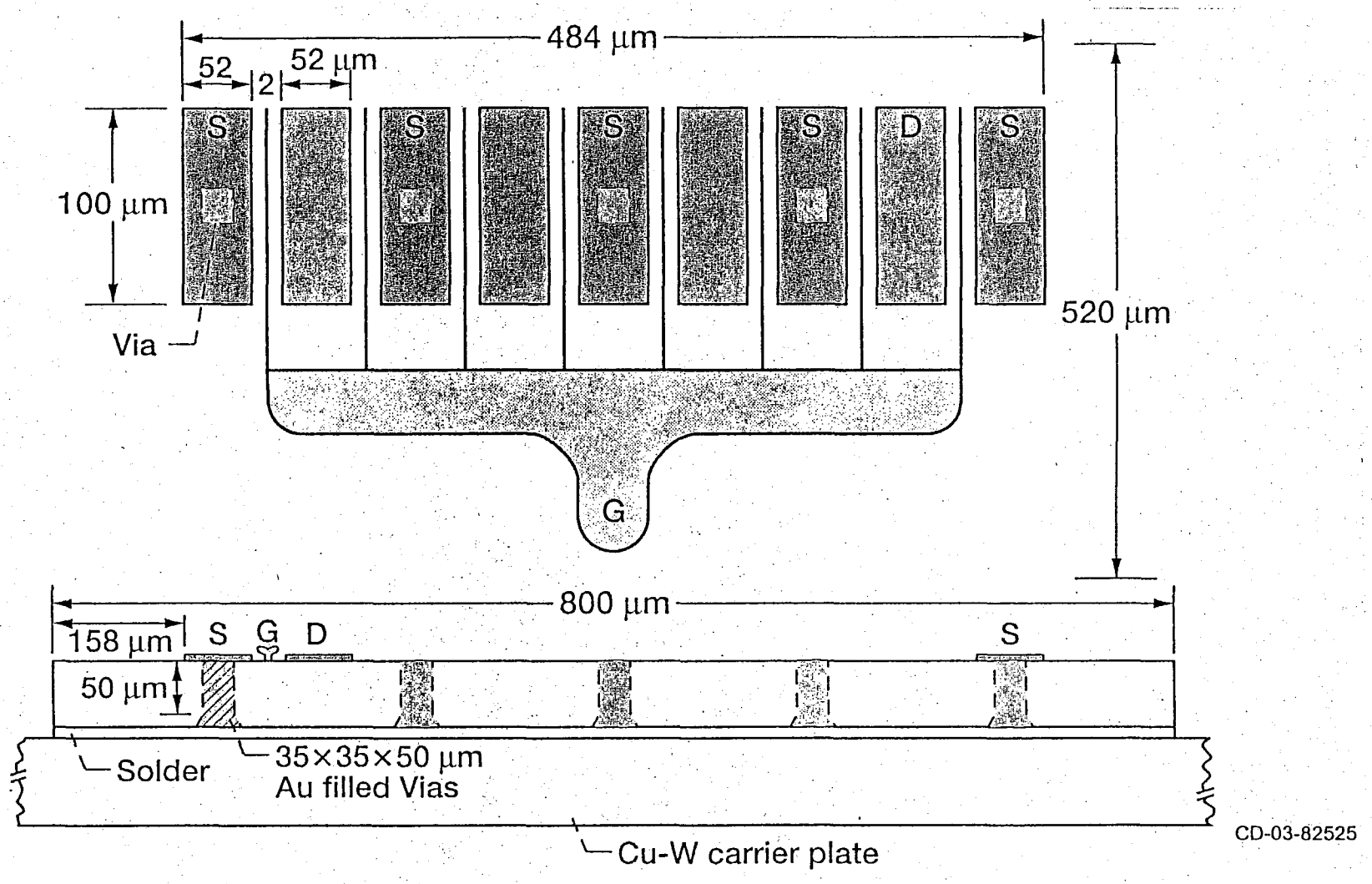

Figure 1 Schematic of an 8-gate HEMT for Ka-band operation.

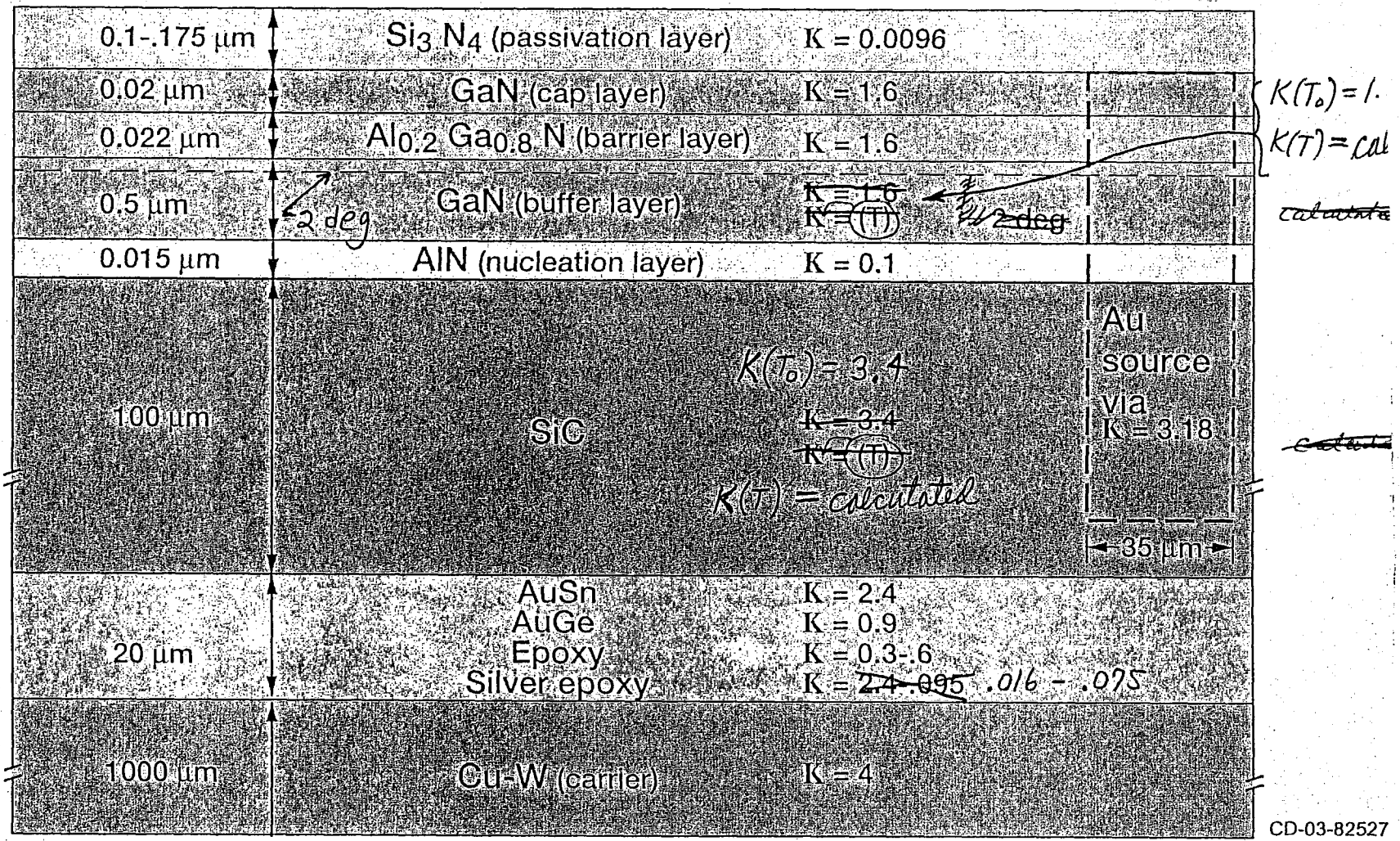

Figure 2 Approximate layers of material with average or ranges of thermal conductivities K.

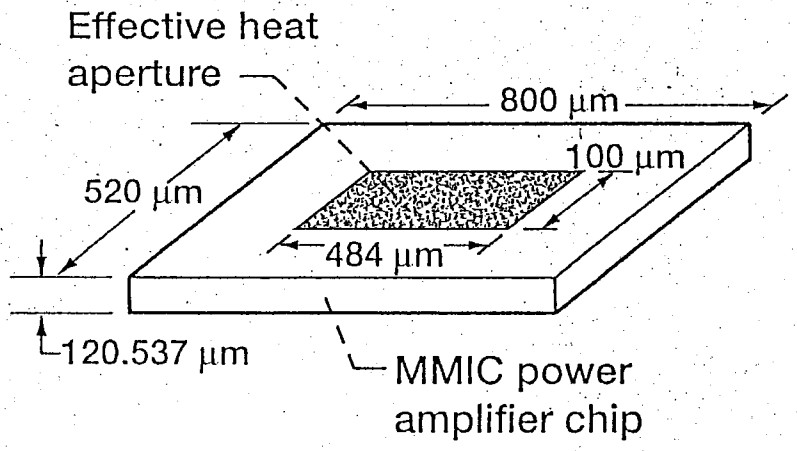

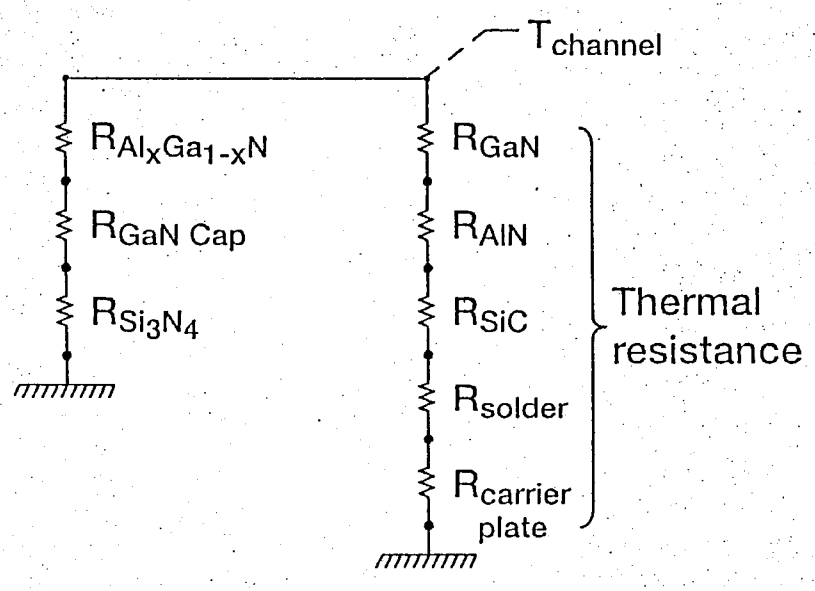

For a typical chip with 8 gate fingers and Lg = 0.15 µm, Wg = 100 µm, gate centered in the source drain gap of 2 µm

Power density, W/mm	Carrier plate temperature, K (°C)	Channel temperature, K (°C)
2	300 (27)	366 (93)
2	350 (77)	415 (142)
2	370 (97)	435 (162)

PAE = 30%

Table I

$T_{channel}$	93 °C
R_{GaN}	56.5 °C/W
R_{AlN}	10.7 °C/W
R_{SiC}	7.67 °C/W
R_{solder}	.525 °C/W
$R_{carrier\ plate}$	.02 °C/W

CD-03-82523

Table II

Figure 3 Device of Figure 1 on an approximate MMIC chip. The thermal resistance of each layer is calculated separately ($\theta \equiv R_{TH}$).

one Table

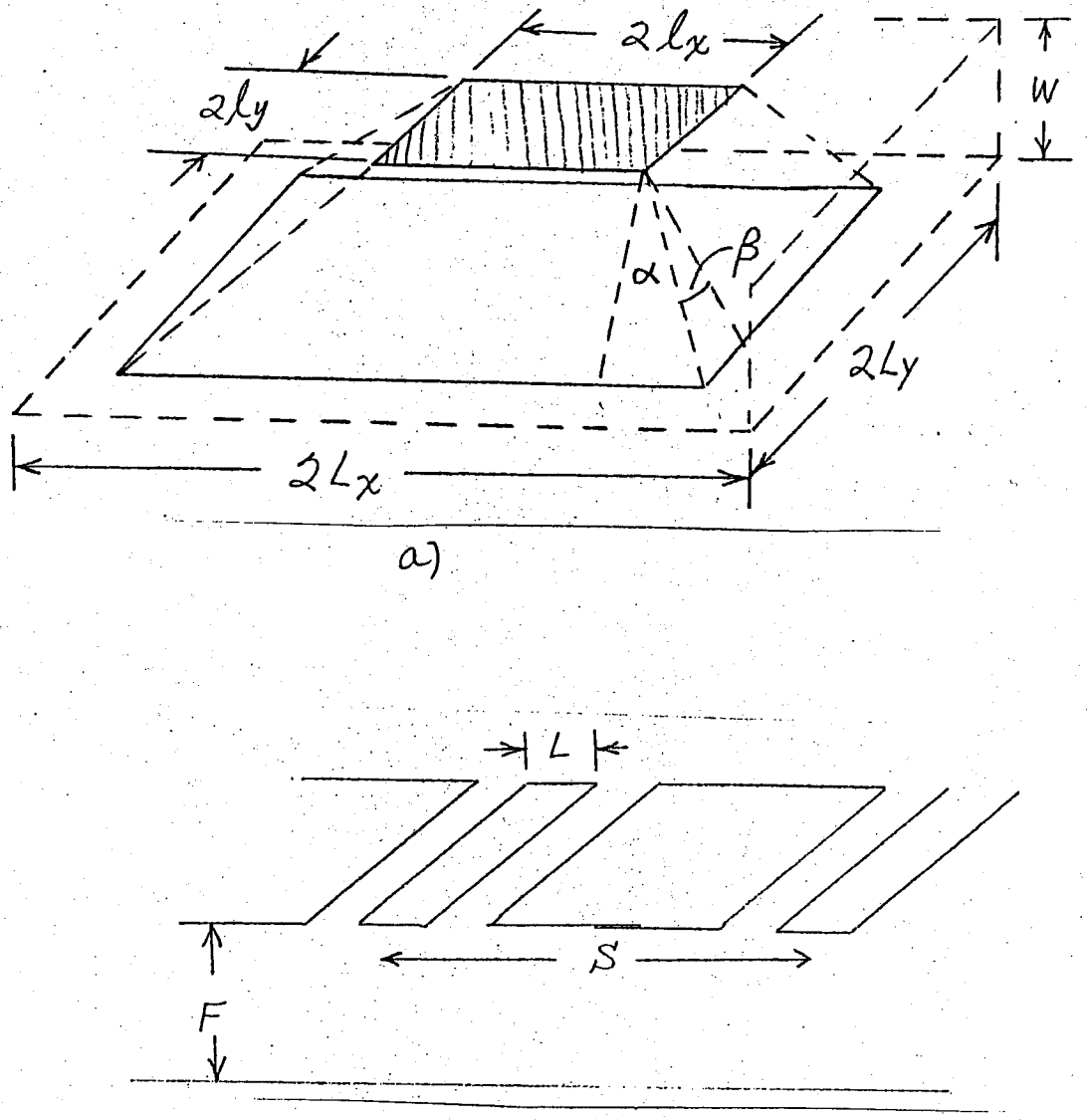

Figure 4 Geometry for calculating thermal resistance for a single stripe a), or parallel stripes b).

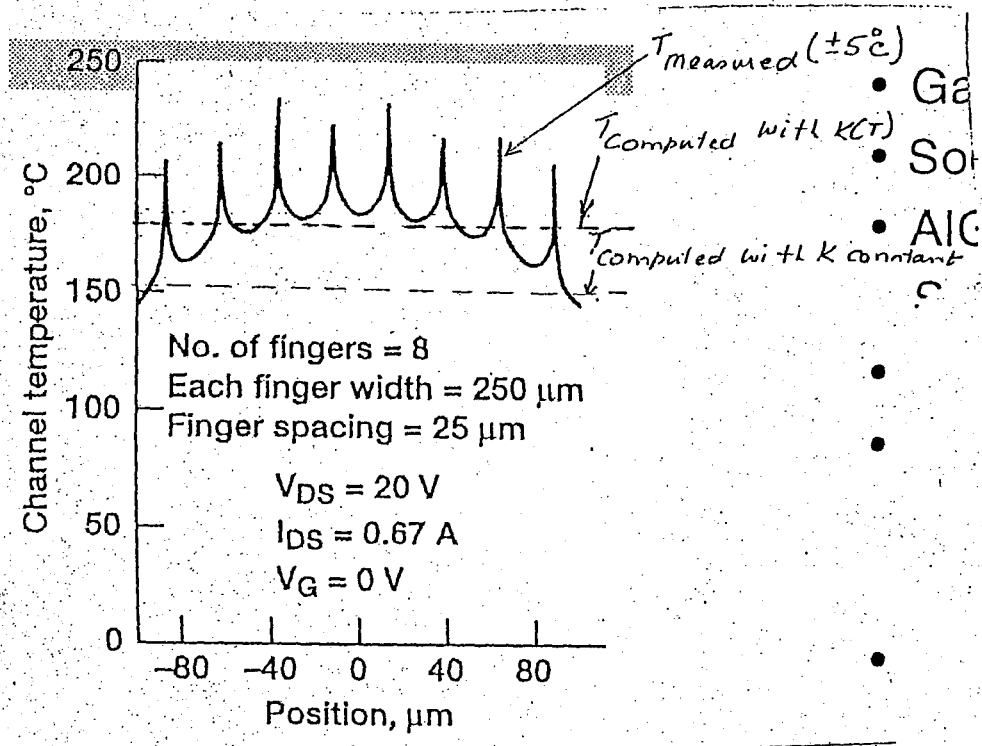

a)

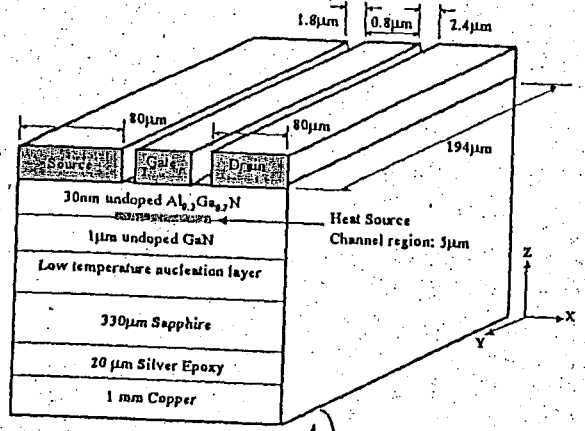

b)

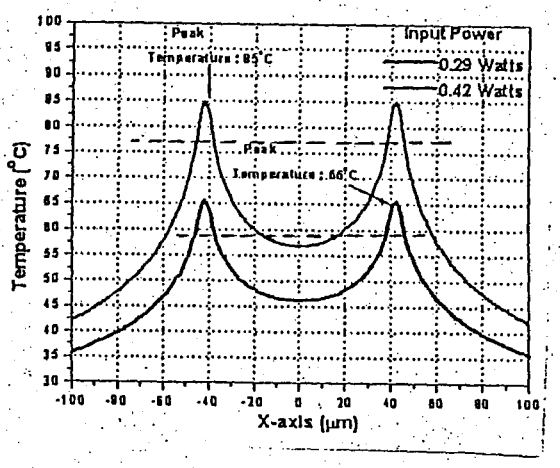

c)

Figure 5 Comparison with Kuball [16] and Park [17]. Part a) shows measurement (solid) and estimate (dotted). Part b) shows estimates (dotted) for two power dissipation cases [17].